Differential Roles of Ionic, Aliphatic, and Aromatic Residues in Membrane−Protein Interactions: A Surface Plasmon Resonance Study on Phospholipases A_2[†]

Robert V. Stahelin and Wonhwa Cho*

Department of Chemistry (M/C 111), University of Illinois at Chicago, 845 West Taylor Street, Chicago, Illinois 60607-7061

Received August 28, 2000; Revised Manuscript Received February 14, 2001

ABSTRACT: The roles of cationic, aliphatic, and aromatic residues in the membrane association and dissociation of five phospholipases A_2 (PLA_2), including Asp-49 PLA_2 from the venom of *Agkistodon piscivorus piscivorus*, acidic PLA_2 from the venom of *Naja naja atra*, human group IIa and V PLA_2s, and the C2 domain of cytosolic PLA_2, were determined by surface plasmon resonance analysis. Cationic interfacial binding residues of *A. p. piscivorus* PLA_2 (Lys-10) and human group IIa PLA_2 (Arg-7, Lys-10, and Lys-16), which mediate electrostatic interactions with anionic membranes, primarily accelerate the membrane association. In contrast, an aliphatic side chain of the C2 domain of cytosolic PLA_2 (Val-97), which penetrates into the hydrophobic core of the membrane and forms hydrophobic interactions, mainly slows the dissociation of membrane-bound protein. Aromatic residues of human group V PLA_2 (Trp-31) and *N. n. atra* PLA_2 (Trp-61, Phe-64, and Tyr-110) contribute to both membrane association and dissociation steps, and the relative contribution to these processes depends on the chemical nature and the orientation of the side chains as well as their location on the interfacial binding surface. On the basis of these results, a general model is proposed for the interfacial binding of peripheral proteins, in which electrostatic interactions by ionic and aromatic residues initially bring the protein to the membrane surface and the subsequent membrane penetration and hydrophobic interactions by aliphatic and aromatic residues stabilize the membrane−protein complexes, thereby elongating the membrane residence time of protein.

Many cellular peripheral proteins are targeted to different subcellular membranes during cell signaling. Also, a number of extracellular proteins, including lipolytic enzymes, interact with cell membranes and lipid aggregates. Since the interfacial binding of these proteins plays a critical role in their function and regulation, extensive efforts have been made to understand the mechanisms and energetics of their interactions with membranes. Phospholipases A_2 (PLA_2)[1] have long been used as a paradigm for these studies, thanks to the wealth of structural and functional information as well as their involvement in inflammation and other important biological processes. PLA_2s catalyze the hydrolysis of fatty acid ester at the *sn*-2 position of phospholipids and are found in both intracellular and secreted forms. Since PLA_2s act on phospholipids in membranes or in other aggregated forms, their interfacial catalysis includes the interfacial binding, which is distinct from the binding of a phospholipid molecule to the active site (*1*, *2*). Secretory PLA_2s ($sPLA_2$s) are small (∼14 kDa), disulfide-rich, Ca^{2+}-dependent enzymes that can be classified into at least 11 groups (*3*). Structural analyses of multiple $sPLA_2$s have led to the proposal of a common interfacial binding surface (IBS) that is located on a flat external surface that surrounds the active site slot (*4*). Subsequent structure−function studies on $sPLA_2$s have identified essential IBS residues, including cationic, aromatic, and aliphatic residues (*5*−*11*). In general, these IBS residues interact with the membrane surface without significant disruption of the hydrophobic core of the membrane (*6*, *11*, *12*). Group IV cytosolic PLA_2 ($cPLA_2$) shares no structural homology to $sPLA_2$s (*13*) and has a distinct interfacial binding mechanism (*12*). The interfacial binding of $cPLA_2$ is mediated by the amino-terminal C2 domain (*14*). The C2 domain is a Ca^{2+}-dependent membrane-targeting domain that is also found in other cellular proteins, a majority of which are involved in membrane binding or membrane trafficking (*15*, *16*). The C2 domain of $cPLA_2$ contains several hydrophobic residues on its putative IBS, which penetrate into the membrane in a calcium-dependent manner during the interfacial binding of $cPLA_2$ (*17*−*19*).

Despite these structural and functional studies on IBS residues of PLA_2s, no specific information is available as to how exactly they affect the membrane association and dissociation steps. In the present study, we studied the roles of three types of IBS residues, cationic, aliphatic, and aromatic, in the interfacial binding of several PLA_2s, including a basic $sPLA_2$ from the venom of *Agkistodon*

[†] This work was supported by NIH Grants GM52598 and GM53987. W.C. is an Established Investigator of American Heart Association.

* To whom correspondence should be addressed. Tel: 312-996-4883. Fax: 312-996-2183. E-mail: wcho@uic.edu.

[1] Abbreviations: App-D49, Asp-49 PLA_2 from *Agkistrodon piscivorus piscivorus*; BSA, bovine serum albumin; $cPLA_2$, cytosolic phospholipase A_2; DHPC, 1,2-di-*O*-hexadecyl-*sn*-glycero-3-phosphocholine; EGTA, ethylene glycol bis(*β*-aminoethyl ether)-*N*,*N*,*N*′,*N*′-tetraacetic acid; $hIIaPLA_2$, human group IIa phospholipase A_2; $hVPLA_2$, human group V phospholipase A_2; IBS, interfacial binding surface; $nnaPLA_2$, *Naja naja atra* phospholipase A_2; PCR, polymerase chain reaction; PLA_2, phospholipase A_2; POPG, 1-palmitoyl-2-oleoyl-*sn*-glycero-3-phosphoglycerol; RU, resonance unit; SPR, surface plasmon resonance.

10.1021/bi0020325 CCC: $20.00 © 2001 American Chemical Society
Published on Web 03/22/2001

piscivorus piscivorus (App-D49), an acidic $sPLA_2$ from the venom of *Naja naja atra* ($nnaPLA_2$), human group IIa $sPLA_2$ ($hIIaPLA_2$), human group V $sPLA_2$ ($hVPLA_2$), and $cPLA_2$ by surface plasmon resonance (SPR) analysis. Results provide new insights into the differential roles of these residues in membrane association and dissociation steps.

MATERIALS AND METHODS

Materials. 1-Palmitoyl-2-oleoyl-*sn*-glycero-3-phosphoglycerol (POPG) was from Avanti Polar Lipids (Alabaster, AL). 1,2-Di-*O*-hexadecyl-*sn*-glycero-3-phosphocholine (DHPC) was from Sigma (St. Louis, MO). Phospholipid concentrations were determined by phosphate analysis (*20*). The Liposofast microextruder and 100 nm polycarbonate filters were from Avestin (Ottawa, Ontario). Fatty acid-free bovine serum albumin (BSA) was from Bayer, Inc. (Kankakee, IL). 3-[(3-Cholamidopropyl)dimethylammonio]-1-propanesulfonate and octyl glucoside were from Sigma and Fisher Scientific, respectively. Pioneer L1 sensor chip was from Biacore AB (Piscataway, NJ).

PLA_2 Expression and Purification. All PLA_2s and mutants, including App-D49 (*7*), $nnaPLA_2$ (*11*), $hIIaPLA_2$ (*8*), $hVPLA_2$ (*10*, *21*), and the C2 domain of $cPLA_2$ (*17*), were expressed in *Escherichia coli* and purified as described previously.

Preparation of Vesicle-Coated Sensor Chips. From lipid stock solutions in chloroform, 400 μg/mL solutions of vesicles were prepared for coating the Pioneer L1 sensor chip. Lipids in chloroform were dried under N_2 in order to remove chloroform and then resuspended in an appropriate flow buffer solution (typically 10 mM HEPES, pH 7.4, containing 0.1 M NaCl and varying concentrations of Ca^{2+}). The solution was then vortexed for 15 min and sonicated for 2 min in a Branson 1200 sonifier. After sonication, vesicles were passed 17 times through a Liposofast microextruder containing a 100 nm polycarbonate filter. Before SPR measurements, the Biacore X (Biacore AB) instrument was allowed to equilibrate with the buffer until the drift in signal was less than 0.3 resonance units (RU)/min. The sensor surface was then coated with lipid vesicles of choice (DHPC or POPG vesicles) at a flow rate of 5 μL/min. Typically, 150 μL of these vesicle solutions was used for coating. The resulting signal from immobilized vesicles was dependent upon the type of lipid vesicle injected; e.g., 4200 RU for POPG and 7100 RU for DHPC vesicles. The immobilized lipid vesicles were washed with 10 μL of 10 mM NaOH at 100 μL/min flow rate to remove unattached vesicles. Typically, no further decrease in SPR signal was observed after one wash cycle. In control experiments, the fluorescence intensity of the flow buffer after rinsing the sensor chip coated with DHPC or POPG vesicles incorporating 10 mM 5-carboxyfluorescien (Molecular Probes) was monitored. Lack of detectable fluorescence signal indicated that the vesicles remained intact on the chip. Next, 25 μL of 0.1 mg/mL BSA was injected at 5 μL/min to block exposed sites on the chip surface, which typically gave rise to 100 RU. This surface was once again washed with 10 mM NaOH. All experiments were performed with a control cell in which a second sensor surface was coated with 0.1 mg/mL BSA at 5 μL/min and then washed with 10 mM NaOH. The typical response from BSA coating was 1200 RU on the control surface and 100 RU on the lipid-coated surface. The drift in signal for both sample and control flow cells was allowed to stabilize below 0.3 RU/min before any kinetic experiments were performed.

SPR Measurements. All SPR experiments were performed at 24 °C and a flow rate of 60 μL/min. A high flow rate was used to circumvent mass transport effects. The association was monitored for 90 s (90 μL) and dissociation for 4 min. The immobilized vesicle surface was then regenerated for subsequent measurements using 10 μL of 10−50 mM NaOH or 3 M NaCl. The regeneration solution was passed over the immobilized vesicle surface until the SPR signal reached the initial background value before protein injection. For data acquisition, five or more different concentrations (typically within a 10-fold range above or below the K_d) of each PLA_2 were used. After each set of measurements, the entire immobilized vesicles were removed by injection of 25 μL of 40 mM 3-[(3-cholamidopropyl)dimethylammonio]-1-propanesulfonate, followed by 25 μL of octyl glucoside at 5 μL/min, and the sensor chip was recoated with a fresh vesicle solution for the next set of measurements. All data were evaluated using BIAevaluation 3.0 software (Biacore). For each trial, the control surface response was subtracted out in order to eliminate any refractive index changes due to buffer change. Furthermore, the derivative plot was used to monitor potential mass transport effects.

Once these factors were checked for each set of data, the association and dissociation phases of all sensorgrams (see Figure 1) were globally fit to a 1:1 Langmuir binding model: [protein·vesicle] ↔ protein + vesicle. The association phase was analyzed using an equation

$$R = [k_a C/(k_a C + k_d)]R_{max}(1 - e^{-(k_a C + k_d)(t - t_0)}) + \mathrm{RI}$$

where RI = refractive index change, R_{max} is the theoretical binding capacity, C is analyte concentration, k_a is the association rate constant, and t_0 is the time at start of fit data. The dissociation phase was analyzed using an equation

$$R = R_0 e^{k_d(t - t_0)}$$

where k_d is the dissociation rate constant and R_0 is the response at the start of fit data. Then, the curve fitting efficiency was checked by residual plots and χ^2. The dissociation constant (K_d) was then calculated from the equation

$$K_d = k_d/k_a$$

RESULTS

Establishing SPR Methodology for Interfacial Binding Analysis. In these studies, we used the SPR technique to elucidate the roles of interfacial binding residues in membrane association and dissociation steps. For this purpose, the SPR technique offers a great advantage over other methods in that the effects of the mutation of these residues on membrane association (k_a) and dissociation (k_d) rate constants can be directly determined (*22*, *23*). As a model membrane, we employed the phospholipid vesicles immobilized on the Pioneer L1 sensor chip. This sensor chip allows direct attachment and immobilization of intact vesicles by means

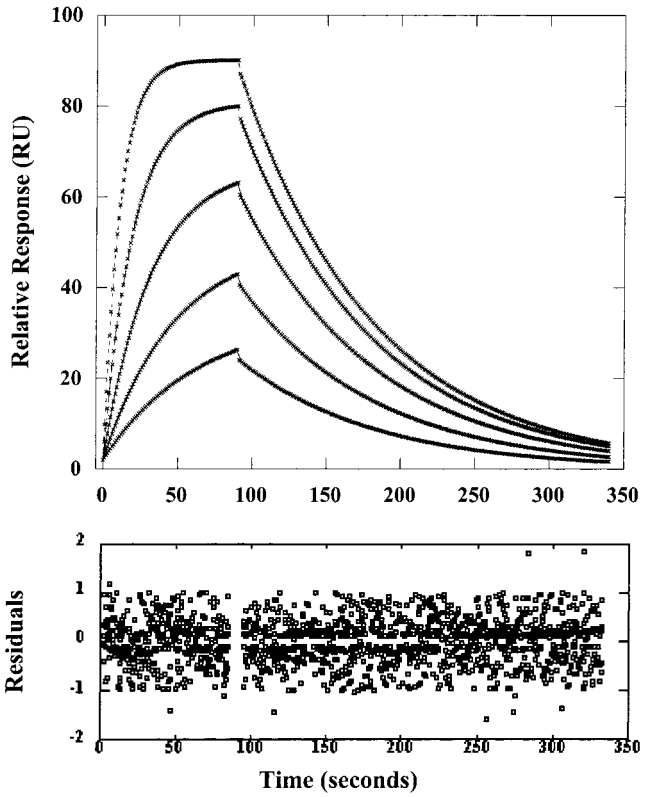

FIGURE 1: Representative sensorgrams for PLA_2-immobilized vesicle binding. The Pioneer L1 chip surface was coated with DHPC vesicles at 5 μL/min in 0.1 mM HEPES, 0.1 M NaCl, and 0.1 mM EGTA. nnaPLA$_2$/F64A (60 μL) of varying concentrations (0.1, 0.2, 0.4, 0.8, and 1.6 μM) was injected at 60 μL/min, and the subsequent association and dissociation were monitored.

of its hydrophobic anchors, thereby removing the need to incorporate anchor molecules in vesicles (*24*). The vesicles immobilized on the sensor chip have been shown to remain intact (*24*). Immobilized DHPC and POPG vesicles also remained intact under our experimental conditions, as evidenced by the lack of vesicle leakage (see Materials and Methods). To circumvent any potential artifacts caused by the hydrophobic nature of commercial L1 chip, e.g., nonspecific protein binding to the chip, both control surface and vesicle-coated surface were treated with BSA. For both surfaces, no appreciable change in SPR response was seen in response to the second injection of BSA, showing that the nonspecific binding sites were essentially all blocked by a single BSA treatment (see, for instance, the binding of C2 domain in the presence and absence of Ca^{2+}). The binding of PLA_2 to BSA was not detected under our experimental conditions, as evidenced by the lack of signal from the control surface when the PLA_2 sample was injected (data not shown). We also controlled refractive index changes upon buffer change and the mass transport effect (*22*, *23*) to minimize the experimental artifacts and the erroneous data analysis in our SPR measurements. The former was compensated for by subtracting the control signal from the sample signal for each measurement. The latter effect depends heavily on two factors, ligand density and flow rate. To prevent the mass transport events, low ligand density and high flow rate were kept at the levels where the rate constants are independent of 2−3-fold variation of these factors. For example, neither the variation of flow rate from 60 to 30 μL/min (see Table 1) nor 3-fold variation of total surface lipid density (1400−4200 RU of POPG) led to significant deviation of rate constants, confirming that mass transport effects have a negligible effect on our kinetic analysis. Figure 1 shows representative sensorgrams for nnaPLA$_2$. The data fit well to a 1:1 Langmuir binding model, as indicated by its low and random residual scatter.

Role of Cationic Residues of App-D49 and hIIaPLA$_2$. Two basic sPLA$_2$s, hIIaPLA$_2$ and App-D49, have high affinity and activity for anionic membranes (*7*, *25*, *26*). These sPLA$_2$s contain cationic residues on their IBSs that play essential roles in interfacial binding to anionic membranes (*7*, *8*). To systematically investigate the role of cationic residues in their interfacial binding, we measured the binding of App-D49, hIIaPLA$_2$, and their mutants to immobilized zwitterionic and anionic vesicles by SPR analysis under different conditions. To avoid the hydrolysis of phospholipids, the binding measurements of sPLA$_2$s were performed either with vesicles made of a nonhydrolyzable phospholipid analogue (i.e., DHPC) or in the absence of Ca^{2+} (for anionic POPG vesicles). The selection of the latter condition was mainly due to the difficulty in preparing a PG analogue of DHPC in an amount sufficient for SPR measurements. First, we measured the binding of wild-type proteins to immobilized POPG vesicles in the absence of Ca^{2+}. We previously showed (*10*, *17*, *25*, *27*) that the binding of App-D49 and hIIaPLA$_2$ (and other sPLA$_2$s used in these studies) to both zwitterionic and anionic membranes does not depend on Ca^{2+} (see also Table 1). Figure 2 shows sensorgrams for high-affinity App-D49-POPG binding. As is the case with Figure 1, the data fit well to a 1:1 Langmuir binding model, as indicated by its low and random residual scatter. The rate constants derived from these plots are summarized in Table 1.

The K_d for App-D49 (19 nM) calculated from k_a and k_d values compares well with the equilibrium dissociation constant determined by the fluorometric analysis (i.e., K_d = 20 nM) (*7*), supporting the validity of our data analysis. For hIIaPLA$_2$, the calculated K_d (=0.13 nM) was significantly lower than the equilibrium dissociation constant determined by the centrifugal analysis (K_d = 1 nM) (*8*), which is presumably due to higher sensitivity of the SPR analysis compared to the centrifugal assay, the sensitivity limit of which is around 1 nM (*8*). The exceptionally high affinity of hIIaPLA$_2$ for immobilized POPG vesicles was mainly due to its high membrane association rate constant, which is 36-fold higher than that of App-D49. The difference in dissociation rate constant between the two proteins was less pronounced (~4-fold).

We then determined the k_a and k_d values for mutants, K10E for App-D49 and R7E/K10E/K16E for hIIaPLA$_2$, both of which were shown to have dramatically reduced affinity for anionic vesicles (*7*, *8*). Consistent with our previously published data (*7*, *8*), K10E and R7E/K10E/K16E had 32-fold and 385-fold lower affinity than their respective wild-type proteins. The decrease in K_d by a single K10E mutation for App-D49 derived solely from the reduced association rate constant. Similarly, the reduced affinity of hIIaPLA$_2$/R7E/K10E/K16E was due in large part to a 55-fold decrease in k_a. These results indicate that the cationic interfacial binding residues enhance interfacial binding mainly by accelerating the membrane adsorption of protein.

Table 1: Binding Parameters[a] for App-D49, $hIIaPLA_2$, and Mutants

enzymes	k_a (M^{-1} s^{-1})	k_d (s^{-1})	K_d (M)
	POPG and 0.1 M NaCl		
App-D49	$(9.0 \pm 0.9) \times 10^4$	$(1.7 \pm 0.2) \times 10^{-3}$	$(1.9 \pm 0.3) \times 10^{-8}$
App-D49 (30 μL/min)[b]	$(8.5 \pm 0.5) \times 10^4$	$(1.5 \pm 0.2) \times 10^{-3}$	$(1.8 \pm 0.2) \times 10^{-8}$
App-D49/K10E	$(2.8 \pm 0.4) \times 10^3$	$(1.7 \pm 0.3) \times 10^{-3}$	$(6.2 \pm 1.4) \times 10^{-7}$
$hIIaPLA_2$	$(3.2 \pm 0.7) \times 10^6$	$(4.2 \pm 0.5) \times 10^{-4}$	$(1.3 \pm 0.3) \times 10^{-10}$
$hIIaPLA_2$/R7E/K10E/K16E	$(5.8 \pm 0.7) \times 10^4$	$(2.9 \pm 0.3) \times 10^{-3}$	$(5.0 \pm 0.8) \times 10^{-8}$
	POPG and 0.5 M NaCl		
App-D49	$(1.0 \pm 0.2) \times 10^3$	$(1.3 \pm 0.4) \times 10^{-3}$	$(1.3 \pm 0.5) \times 10^{-6}$
App-D49/K10E	$(1.3 \pm 0.3) \times 10^2$	$(1.3 \pm 0.6) \times 10^{-3}$	$(7.2 \pm 3.7) \times 10^{-6}$
$hIIaPLA_2$	$(3.5 \pm 0.7) \times 10^4$	$(2.6 \pm 0.2) \times 10^{-3}$	$(7.4 \pm 1.6) \times 10^{-8}$
$hIIaPLA_2$/R7E/K10E/K16E	$(2.5 \pm 0.2) \times 10^3$	$(2.3 \pm 0.4) \times 10^{-3}$	$(9.2 \pm 1.8) \times 10^{-7}$
	DHPC and 0.1 M NaCl		
$hIIaPLA_2$ (no Ca^{2+})	$(2.2 \pm 0.4) \times 10^4$	$(1.4 \pm 0.5) \times 10^{-3}$	$(6.4 \pm 2.6) \times 10^{-8}$
$hIIaPLA_2$ (5 mM Ca^{2+})	$(2.4 \pm 0.3) \times 10^4$	$(1.8 \pm 0.7) \times 10^{-3}$	$(7.6 \pm 3.1) \times 10^{-8}$

[a] Parameters represent mean ± SD from five or more determinations. [b] Measured at a reduced flow rate.

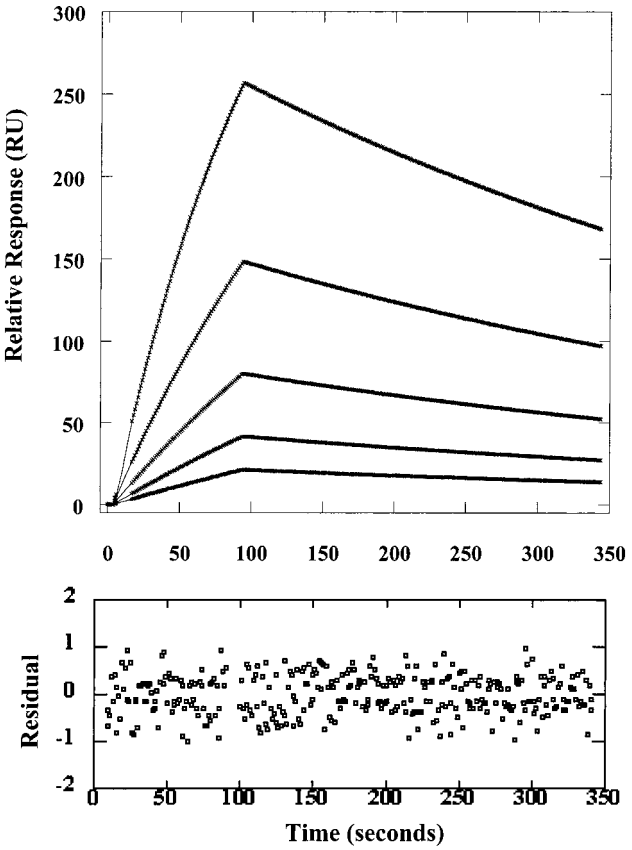

FIGURE 2: Sensorgrams for App-D49 binding to immobilized POPG vesicles. The Pioneer L1 chip surface was coated with POPG vesicles at 5 μL/min in 0.1 mM HEPES, 0.1 M NaCl, and 0.1 mM EGTA. App-D49 (60 μL) of varying concentrations (5, 10, 20, 40, and 80 nM) was injected at 60 μL/min, and the subsequent association and dissociation were monitored. Control flow cell data were then subtracted from each curve for data analysis.

We have previously shown that electrostatic interactions play a predominant role in the binding of App-D49 and $hIIaPLA_2$ to anionic membranes (*7*, *8*). To determine exactly how electrostatic interactions influence the interfacial binding, we measured the effect of the ionic strength on the membrane association and dissociation. An initial attempt to increase the NaCl concentration from 0.1 to 1 M NaCl was hampered by an extremely low degree of binding at 1 M NaCl (e.g., $k_a \ll 10^3$ M^{-1} s^{-1}). To achieve an adequate degree of binding for kinetic analysis, the NaCl concentration was therefore adjusted to 0.5 M NaCl, and the values of k_a and k_d were determined for App-D49, $hIIaPLA_2$, and mutants (see Table 1). Clearly, high ionic strength mainly influenced the association step. The effect on dissociation was insignificant except for the 7-fold decrease seen for $hIIaPLA_2$. As expected from the mutations of essential cationic IBS residues, K10E of App-D49 and R7E/K10E/K16E of $hIIaPLA_2$ were influenced by the high ionic strength to much lesser degrees than their respective wild-type proteins. As a result, differences in both k_a and K_d between wild type and mutants were much smaller at 0.5 M NaCl than at 0.1 M NaCl. Thus, it is evident that the primary role of electrostatic interactions mediated by cationic interfacial binding residues is to drive the membrane association.

To further investigate the role of electrostatic interactions in interfacial binding, we measured the kinetics of binding of $hIIaPLA_2$ to immobilized DHPC vesicles. App-D49 was not included in these measurements because of its extremely low affinity for PC membranes. In these studies, the binding was measured both in the presence of 5 mM Ca^{2+} and in the absence of Ca^{2+}. As listed in Table 1, Ca^{2+} did not have significant effects on the rate of association and dissociation, again validating our Ca^{2+}-free method used for POPG binding. When compared under the same conditions, $hIIaPLA_2$ bound immobilized PC vesicles 146 times slower than immobilized POPG vesicles. In contrast, differences in k_d were only 3.3-fold for $hIIaPLA_2$. Thus, these results again support the notion that electrostatic interfacial interactions mainly facilitate the membrane association.

Role of Aromatic Residues of $hVPLA_2$ and $nnaPLA_2$. Mammalian group V PLA_2s, including $hVPLA_2$, have been shown to have high affinity and activity for zwitterionic PC membranes, including the outer plasma membranes of mammalian cells (*10*, *21*). This is in sharp contrast to homologous group IIa PLA_2s (e.g., $hIIaPLA_2$) that show extremely low activity on PC membranes (*8*, *26*, *28*). Also, acidic PLA_2s from cobra venom, including $nnaPLA_2$, have been shown to have high activity on PC membranes (*11*). We have recently shown that aromatic residues on their interfacial binding surfaces, Trp in particular, play a key role in their high affinity for PC membranes (*2*, *10*, *11*). To further investigate the role of the aromatic residues in interfacial binding, we determined the membrane binding parameters for $hVPLA_2$, $nnaPLA_2$, and their mutants by SPR analysis.

Table 2: Binding Parameters[a] for hVPLA$_2$, nnaPLA$_2$, and Mutants

enzymes	k_a (M^{-1} s^{-1})	k_d (s^{-1})	K_d (M)
		DHPC	
hVPLA$_2$	$(9.1 \pm 0.8) \times 10^5$	$(1.0 \pm 0.3) \times 10^{-3}$	$(1.1 \pm 0.4) \times 10^{-9}$
hVPLA$_2$/W31A	$(1.4 \pm 0.4) \times 10^5$	$(2.7 \pm 0.5) \times 10^{-3}$	$(1.9 \pm 0.6) \times 10^{-8}$
nnaPLA$_2$	$(7.6 \pm 0.6) \times 10^5$	$(1.4 \pm 0.4) \times 10^{-3}$	$(1.8 \pm 0.5) \times 10^{-9}$
nnaPLA$_2$/W61A	$(2.4 \pm 0.6) \times 10^4$	$(6.7 \pm 0.8) \times 10^{-3}$	$(2.6 \pm 0.7) \times 10^{-7}$
nnaPLA$_2$/F64A	$(5.1 \pm 0.5) \times 10^4$	$(1.1 \pm 0.4) \times 10^{-2}$	$(2.2 \pm 0.8) \times 10^{-7}$
nnaPLA$_2$/Y110A	$(1.5 \pm 0.3) \times 10^5$	$(5.0 \pm 0.2) \times 10^{-3}$	$(3.3 \pm 0.7) \times 10^{-8}$
		POPG	
hVPLA$_2$	$(2.9 \pm 0.9) \times 10^6$	$(2.7 \pm 0.2) \times 10^{-4}$	$(9.3 \pm 3.0) \times 10^{-11}$
hVPLA$_2$/W31A	$(5.6 \pm 0.7) \times 10^5$	$(4.5 \pm 0.6) \times 10^{-4}$	$(8.0 \pm 1.5) \times 10^{-10}$
nnaPLA$_2$	$(4.1 \pm 0.5) \times 10^4$	$(1.9 \pm 0.3) \times 10^{-4}$	$(4.8 \pm 0.9) \times 10^{-9}$
nnaPLA$_2$/W61A	$(1.6 \pm 0.3) \times 10^4$	$(1.5 \pm 0.2) \times 10^{-3}$	$(9.4 \pm 2.2) \times 10^{-8}$
nnaPLA$_2$/F64A	$(3.3 \pm 0.4) \times 10^4$	$(1.2 \pm 0.3) \times 10^{-3}$	$(3.6 \pm 1.0) \times 10^{-8}$
nnaPLA$_2$/Y110A	$(4.4 \pm 0.3) \times 10^4$	$(6.4 \pm 0.4) \times 10^{-4}$	$(1.5 \pm 0.1) \times 10^{-8}$

[a] Parameters represent mean ± SD from five or more determinations. All measurements were performed with 0.1 M NaCl and 0.1 mM EGTA.

As summarized in Table 2, hVPLA$_2$ had 36-fold higher affinity for immobilized DHPC vesicles than hIIaPLA$_2$, which was mainly ascribed to the 24-fold larger k_a value. Similarly, nnaPLA$_2$ showed the high PC affinity due to faster adsorption to PC vesicles. We previously reported that mutations of the aromatic residues on the interfacial binding surfaces of these enzymes had large effects on their PC affinity (*10*, *11*). In agreement of these findings, our SPR analysis showed that the mutations resulted in 20−150-fold reduction in PC affinity. The mutations influenced both k_a and k_d values, although changes in k_a were in general larger than those in k_d. Thus, it appears that the aromatic interfacial residues not only accelerate the membrane adsorption but also elongate the membrane residence time.

We then measured the binding of wild type and mutant proteins to immobilized POPG vesicles. As reported previously, hVPLA$_2$ showed significantly (12-fold) higher affinity for anionic POPG vesicles than for PC vesicles whereas nnaPLA$_2$ exhibited slightly (2.7-fold) lower affinity for anionic vesicles (*10*, *11*). The increased affinity of hVPLA$_2$ for POPG vesicles might be due to several cationic residues on its IBS. For POPG vesicles, the effects of W31A mutation of hVPLA$_2$ on k_a and k_d were comparable to those seen with DHPC vesicles. This suggests that Trp-31 plays essentially the same role in binding to the two types of vesicles and that hVPLA$_2$ binds to the vesicles in similar modes. In contrast, nnaPLA$_2$ appears to bind to POPG and DHPC vesicles in different modes for two reasons. First, both association and dissociation of wild type were slower for PG vesicles than for PC vesicles, i.e., 19 times and 7 times reduction in k_a and k_d, respectively. Second, for three mutants the decreases in k_a for POPG vesicles were significantly smaller than those seen for DHPC vesicles, whereas the increases in k_d were comparable for the two types of vesicles.

Role of Hydrophobic Residues of the C2 Domain of cPLA$_2$. The amino-terminal C2 domain of cPLA$_2$ is responsible for its Ca^{2+}-dependent membrane binding. We (*12*, *17*) and others (*18*, *19*) have shown that hydrophobic residues in the C2 domain, including Val-97, are involved in membrane penetration and hydrophobic interactions. To further study the role of hydrophobic residues in interfacial binding, we determined the membrane association and dissociation kinetics of the isolated C2 domain of cPLA$_2$ as well as the C2 domains carrying V97A and M38A mutations, respectively. M38A was used as a negative control since this mutation was shown to have only a modest effect on the interfacial binding of cPLA$_2$ (*17*). For these studies, binding to both DHPC and POPG vesicles were performed in the presence of 0.5 mM Ca^{2+} because the C2 domain requires Ca^{2+} for the membrane binding and has no hydrolytic activity. In the absence of Ca^{2+}, the injection of the C2 domain did not increase the SPR signal beyond the refractive index change, again showing that the SPR signal arose from the specific vesicle binding of protein. As shown in Table 3, the C2 domain of cPLA$_2$ had high affinity for immobilized DHPC vesicles, which was comparable to that of hVPLA$_2$ (see Table 2). The mutation of Val-97 to Ala led to a large 37-fold increase in k_d and a much smaller 3-fold decrease in k_a. This is in sharp contrast to the effects of mutations of cationic interfacial binding residues of App-D49 and hIIaPLA$_2$, which primarily reduced k_a. Unlike V97A, M38A exhibited a modest 4-fold reduction in k_a and only a 20% increase in k_d. As previously reported, the C2 domain had significantly (11-fold) lower affinity for anionic POPG vesicles, which is mainly due to the slower association rate. For these vesicles, the effect of V97A on k_d was much less pronounced (6-fold increase), suggesting that the C2 domain might bind to POPG vesicles in a different orientation that does not allow optimal membrane penetration of Val-97.

Table 3: Binding Parameters[a] for the C2 Domain of cPLA$_2$ and Mutants

enzymes	k_a (M^{-1} s^{-1})	k_d (s^{-1})	K_d (M)
		DHPC	
wild type	$(4.9 \pm 0.3) \times 10^5$	$(1.8 \pm 0.4) \times 10^{-3}$	$(3.6 \pm 0.8) \times 10^{-9}$
M38A	$(1.3 \pm 0.8) \times 10^5$	$(2.1 \pm 0.8) \times 10^{-3}$	$(1.6 \pm 1.2) \times 10^{-8}$
V97A	$(1.8 \pm 0.4) \times 10^5$	$(6.7 \pm 0.5) \times 10^{-2}$	$(3.7 \pm 0.9) \times 10^{-7}$
		POPG	
wild type	$(3.7 \pm 0.8) \times 10^4$	$(1.4 \pm 0.6) \times 10^{-3}$	$(3.8 \pm 1.8) \times 10^{-8}$
M38A	$(1.8 \pm 0.2) \times 10^4$	$(1.2 \pm 0.3) \times 10^{-3}$	$(6.7 \pm 1.8) \times 10^{-8}$
V97A	$(3.0 \pm 0.3) \times 10^4$	$(8.2 \pm 0.6) \times 10^{-3}$	$(2.7 \pm 0.3) \times 10^{-7}$

[a] Parameters represent mean ± SD from five or more determinations. All measurements were performed with 0.1 M NaCl and 0.5 mM Ca^{2+}.

DISCUSSION

It has been generally thought that electrostatic and hydrophobic interactions, mediated by ionic and aliphatic residues, are major driving forces for interfacial binding of PLA$_2$s. More recently, complex interactions between aromatic residues and membranes have also emerged as an

important factor for interfacial binding (*2*, *11*). Although kinetics of membrane association and dissociation of $sPLA_2$s have been measured by different physical techniques (*1*), no systematic study has been reported on the differential roles of cationic, aliphatic, and aromatic IBS residues of PLA_2 in membrane association and dissociation. For protein−protein interactions, the association step is characterized by second-order rate constants (i.e., k_a) that are typically in the range of $(0.5-5) \times 10^6$ M^{-1} s^{-1} (*29*). This value, albeit lower than the diffusion limit (7×10^9 M^{-1} s^{-1}), is 1000−10 000-fold higher than the expected value when strict orientation factors for highly specific protein−protein interactions are considered (*29*). The rapid protein association has been accounted for by different theoretical models, including a lengthy collision model (*30*) and a Brownian dynamics model (*29*). For the ligand binding of human growth hormone receptor, attractive electrostatic forces were shown to enhance the association rate (*31*). Interestingly, however, those human growth hormone residues that are critical for its affinity for receptor binding primarily lowered the dissociation rate without affecting the association rate. On the basis of these data, it was proposed that the initial formation of an ensemble of weak, relatively nonspecific collisional complexes, driven by diffusion and electrostatic forces, is followed by the formation of tightly bound complexes, which are stabilized by a small number of specific interactions, including Coulombic and hydrophobic interactions and hydrogen bonds (*31*). Our data on membrane−protein interactions are in general consistent with this model for protein−protein interactions; yet there are some noticeable differences between the two systems.

Many $sPLA_2$s, $hIIaPLA_2$ in particular, prefer anionic membranes to zwitterionic ones due to the presence of cationic residues on their IBS. k_a values for the binding of App-D49, $hIIaPLA_2$, and $hVPLA_2$ to POPG vesicles (at 0.1 M NaCl) range from 0.1 to 3.2×10^6 M^{-1} s^{-1}, which are comparable to those for protein−protein association. Thus, the association of basic $sPLA_2$s to anionic membranes is as rapid as protein−protein association. Our results show that the membrane association step is primarily driven by electrostatic interactions mediated by cationic IBS residues. We have previously shown that $hIIaPLA_2$ has a large number of cationic IBS residues that collectively contribute to the energetics of interfacial binding (*26*) whereas App-D49 contains a small number of critical cationic IBS residues, including Lys-7 and Lys-10 (*7*). In accordance with the difference in the strength of electrostatic forces, $hIIaPLA_2$ has 35-fold larger k_a than App-D49. Also, a major difference is found between the two proteins in terms of relative contribution of each cationic IBS residue and interfacial binding mechanism. In the case of App-D49, a single charge-reversal mutation (K10E) exerts a large effect (32-fold decrease) on k_a. In contrast, single charge-reversal mutations of the cationic IBS residues of $hIIaPLA_2$ have only modest effects on k_a (not shown) and K_d (*8*): only multiple-site mutations, such as R7E/K10E/K16E, show larger than 10-fold reduction in k_a. This difference also suggests different membrane association mechanisms for the two $sPLA_2$s. The dramatic effect of K10E mutation suggests that the pathways leading to membrane association of App-D49 are limited in number and likely involve Lys-10. For $hIIaPLA_2$, however, there might be multiple pathways leading to membrane association (i.e., the protein can make initial contact with the membrane in different orientations). For both proteins, the mutations mainly influence the membrane association. In the case of App-D49, the K10E mutation exclusively affects k_a, indicating that Lys-10 is involved not in specifically stabilizing the membrane−protein complexes but in interacting *nonspecifically* with the anionic membrane surfaces. For $hIIaPLA_2$, the R7E/K10E/K16E mutation has a considerable effect (7-fold increase) on k_d, albeit smaller than 55-fold decrease in k_a. Similarly, raising the NaCl concentration to 0.5 M increases the k_d for $hIIaPLA_2$ by a factor of 6, while having no effect on that for App-D49. Thus, cationic IBS residues of $hIIaPLA_2$ might also be involved in stabilizing the membrane−protein complexes. However, the effect on k_d could be due to the change in the membrane binding orientation of $hIIaPLA_2$ caused by the triple-site mutation. The introduction of three clustered anionic residues to the cationic IBS of $hIIaPLA_2$ might discriminate against its productive membrane binding orientations, which in turn could interfere with the stabilizing interactions of other residues with the membrane and thereby facilitate the membrane desorption. Taken together, our results indicate that cationic residues of $sPLA_2$s mainly contribute to the membrane association step by nonspecifically interacting with the anionic membrane surfaces.

For hydrophobic side chains of protein to interact with the membrane, they must penetrate into the hydrophobic core of the membrane. In general, the interfacial binding of $sPLA_2$s does not involve a significant degree of membrane penetration. As a result, individual hydrophobic residues do not make large contributions to membrane affinity (*6*). Rather, they contribute collectively to overall interfacial affinity. In contrast, Leu-39 and Val-97 in the calcium binding loops of the C2 domain of $cPLA_2$ have been shown to fully penetrate into the membrane and form hydrophobic interactions (*17*). These residues thus serve as an excellent model to study the role of hydrophobic interactions in membrane association and dissociation. The large 35-fold reduction in k_d by a single V97A mutation demonstrates that the main role of hydrophobic interactions is to stabilize the tight membrane−protein complexes and thereby slow the dissociation of membrane-bound protein. The specific nature of these hydrophobic interactions is verified by the negligible change in k_d caused by the mutation of Met-38 that is located in the vicinity of Leu-39 and Val-97 but does not penetrate into the membrane (*17*).

Unlike the mutations of ionic and aliphatic residues that primarily affect k_a and k_d, respectively, all mutations of aromatic residues of $hVPLA_2$ and $nnaPLA_2$ influence both k_a and k_d, indicating that aromatic side chains play more complex roles in interfacial binding. It has been shown for transmembrane proteins that Trp and Tyr are enriched near the ends of the transmembrane helices whereas Phe is more frequently found in the core of the helices (*32*, *33*). Also, the interactions of Trp with the membrane have been shown to involve a wide variety of electrostatic and nonelectrostatic interactions (*34*). $hVPLA_2$ and $nnaPLA_2$ have much higher (>30-fold) affinity for zwitterionic PC membranes than $hIIaPLA_2$ mainly because of their higher k_a values (see Tables 1 and 2). For $hVPLA_2$, the mutation of a single Trp on its putative IBS (Trp-31) to Ala resulted in ∼7-fold reduction in k_a and ∼3-fold increase in k_d for PC vesicles, indicating

that Trp-31 plays an important role in rapid association to PC membranes. The effect on k_a should be due to electrostatic forces on the basis of the discussion described above. It is likely that the k_d effect, which is less prominent than the k_a effect, also derives from electrostatic forces, given the preference of the Trp side chain for the water−lipid interface. The mutations of nnaPLA$_2$ provide further insights into the differential roles of aromatic residues in membrane association and dissociation. The IBS of nnaPLA$_2$ contains six aromatic residues with different side chain orientations (*35*). Our previous structure−function study on nnaPLA$_2$ showed that Trp-61 and Phe-64 are critical for its binding to PC membranes, whereas Tyr-110 makes less contribution because of its suboptimal location and side chain orientation (*11*). The study also indicated that Trp-61 stays at the lipid−water interface whereas Phe-64 penetrates into the membrane. In agreement of this notion, our results show that Trp-61 contributes predominantly to the membrane association step whereas Phe-64 contributes evenly to both association and dissociation steps. The effect of W61A mutation on k_a (i.e., 36-fold decrease) is ∼5-fold higher than that of W31A mutation of hVPLA$_2$, which might be due to better positioning of W61A on IBS. When compared to the W61A mutation, the F64A mutation results in a smaller 15-fold decrease in k_a but a larger 11-fold increase in k_d, thereby reducing the overall affinity to comparable degrees. Taken together, these results clearly demonstrate differential functions of aromatic side chains in interfacial binding due to their different intrinsic preference for different parts of membranes.

On the basis of these results in conjunction with our previous studies, we propose a general model for membrane binding of peripheral proteins. In this model, electrostatic interactions, whether they are Coulombic interactions between cationic IBS residues (or divalent ion such as Ca^{2+}) and anionic membranes or complex interactions between aromatic residues and zwitterionic membranes, initially bring the protein molecules to the membrane surface, leading to an ensemble of loosely membrane-bound proteins. The subsequent membrane penetration of aliphatic and aromatic residues results in the formation of tight membrane−protein complexes, which are stabilized primarily by hydrophobic interactions and could be further stabilized by electrostatic interactions and hydrogen bonds. For aromatic residues, the chemical nature and the orientation of the side chains as well as their location are important factors governing their differential roles in interfacial binding.

REFERENCES

1. Jain, M. K., and Berg, O. G. (1989) *Biochim. Biophys. Acta 1002*, 127−156.
2. Gelb, M. H., Cho, W., and Wilton, D. C. (1999) *Curr. Opin. Struct. Biol. 9*, 428−432.
3. Valentin, E., and Lambeau, G. (2000) *Biochim. Biophys. Acta 1488*, 59−70.
4. Scott, D. L., and Sigler, P. B. (1994) *Adv. Protein Chem. 45*, 53−88.
5. Dua, R., Wu, S. K., and Cho, W. (1995) *J. Biol. Chem. 270*, 263−268.
6. Lee, B.-I., Yoon, E. T., and Cho, W. (1996) *Biochemistry 35*, 4231−4240.
7. Han, S.-K., Yoon, E. T., Scott, D. L., Sigler, P. B., and Cho, W. (1997) *J. Biol. Chem. 272*, 3573−3582.
8. Snitko, Y., Koduri, R., Han, S.-K., Othman, R., Baker, S. F., Molini, B. J., Wilton, D. C., Gelb, M. H., and Cho, W. (1997) *Biochemistry 36*, 14325−14333.
9. Snitko, Y., Han, S. K., Lee, B. I., and Cho, W. (1999) *Biochemistry 38*, 7803−7810.
10. Han, S. K., Kim, K. P., Koduri, R., Bittova, L., Munoz, N. M., Leff, A. R., Wilton, D. C., Gelb, M. H., and Cho, W. (1999) *J. Biol. Chem. 274*, 11881−11888.
11. Sumandea, M., Das, S., Sumandea, C., and Cho, W. (1999) *Biochemistry 38*, 16290−16297.
12. Lichtenbergova, L., Yoon, E. T., and Cho, W. (1998) *Biochemistry 37*, 14128−14136.
13. Leslie, C. C. (1997) *J. Biol. Chem. 272*, 16709−16712.
14. Nalefski, E. A., Sultzman, L. A., Martin, D. M., Kriz, R. W., Towler, P. S., Knopf, J. L., and Clark, J. D. (1994) *J. Biol. Chem. 269*, 18239−18249.
15. Nalefski, E. A., and Falke, J. J. (1996) *Protein Sci. 5*, 2375−2390.
16. Rizo, J., and Sudhof, T. C. (1998) *J. Biol. Chem. 273*, 15879−15882.
17. Bittova, L., Sumandea, M., and Cho, W. (1999) *J. Biol. Chem. 274*, 9665−9672.
18. Ball, A., Nielsen, R., Gelb, M. H., and Robinson, B. H. (1999) *Proc. Natl. Acad. Sci. U.S.A. 96*, 6637−6642.
19. Nalefski, E. A., and Falke, J. J. (1998) *Biochemistry 37*, 17642−17650.
20. Kates, M. (1986) *Techniques of Lipidology*, 2nd ed., Elsevier, Amsterdam.
21. Han, S.-K., Yoon, E. T., and Cho, W. (1998) *Biochem. J. 331*, 353−357.
22. Myszka, D. G. (1997) *Curr. Opin. Biotechnol. 8*, 50−57.
23. Schuck, P. (1997) *Annu. Rev. Biophys. Biomol. Struct. 26*, 541−566.
24. Cooper, M. A., Hansson, A., Lofas, S., and Williams, D. H. (2000) *Anal. Biochem. 277*, 196−205.
25. Kim, Y., Lichtenbergova, L., Snitko, Y., and Cho, W. (1997) *Anal. Biochem. 250*, 109−116.
26. Snitko, Y., Yoon, E. T., and Cho, W. (1997) *Biochem. J. 321*, 737−741.
27. Han, S.-K., Lee, B.-I., and Cho, W. (1997) *Biochim. Biophys. Acta 1346*, 185−192.
28. Koduri, R., Baker, S. F., Snitko, Y., Han, S.-K., Cho, W., Wilton, D. C., and Gelb, M. H. (1998) *J. Biol. Chem. 273*, 32142−32153.
29. Northrup, S. H., and Erickson, H. P. (1992) *Proc. Natl. Acad. Sci. U.S.A. 89*, 3338−3342.
30. Sommer, J., Jonah, C., Fukuda, R., and Bersohn, R. (1982) *J. Mol. Biol. 159*, 721−744.
31. Cunningham, B. C., and Wells, J. A. (1993) *J. Mol. Biol. 234*, 554−563.
32. Wallin, E., Tsukihara, T., Yoshikawa, S., von Heijne, G., and Elofsson, A. (1997) *Protein Sci. 6*, 808−815.
33. Braun, P., and von Heijne, G. (1999) *Biochemistry 38*, 9778−9782.
34. Yau, W. M., Wimley, W. C., Gawrisch, K., and White, S. H. (1998) *Biochemistry 37*, 14713−14718.
35. White, S. T., Scott, D. L., Otwinowski, Z., Gelb, M. H., and Sigler, P. B. (1990) *Science 250*, 1560−1563.

BI0020325